

MEMOIRS OF THE KOKUSHIKAN UNIVERSITY CENTER FOR INFORMATION SCIENCE

No. 30

March, 2009

CONTENTS

Paper

Geometrical Characterization of Textures Consisting of Two or Three
Discrete Colorings

..... YOSHINORI NAGAI, STEPHEN T. HYDE,
RYAN R. L. TAYLOR and TED MADDESS(1)

Note

A Mathematical Procedure of for the Evaluation of Administered
Medicine Using Measured Data of Cytokine Productivity

..... MASASHI KITO and YOSHINORI NAGAI(14)

Other

Some aspects of e-Learning

..... JOJI TSUKAMOTO and MASAO NAKANE(23)

Memorial Bibliography of Kazuhide Mori

..... HIROSHI KAGAWA and YOSHINORI NAGAI(46)

The Fourth Workshop on e-Learning System

Foreword (53)

A Real Time Questionnaire for e-Learning System

..... TAISUKE KOBAYASHI(55)

A Trial of Faculty Development by Means of Mobile Telephones
and Other Tools

..... TAKAYUKI KISAKA(61)

Usage of Handing Out the Educational Materials for Students and
Reconsideration of Educational Efficiency on the Study of
Subjects Concerning to Using Computers

..... YOSHINORI NAGAI(72)

国士館大学

情報科学センター紀要

第30号

論文

- Geometrical Characterization of Textures Consisting of Two or Three Discrete ColoringsYOSHINORI NAGAI, STEPHEN T. HYDE, RYAN R. L. TAYLOR and TED MADDESS (1)

ノート

- サイトカイン産生能・分泌量測定値を用いた投薬効果検証の為のデータ処理法鬼頭 政, 永井 喜則 (14)

その他

- eラーニングに関する諸相塚本 丞治, 中根 雅夫 (23)
追悼 森和英永井 喜則, 香川 浩 (46)

第四回 e-Learning 研究会報告

- 序文 (53)
講義支援システムなどを利用したリアルタイムアンケートについて …小林 泰介 (55)
携帯電話等を利用したFDの試み木阪 貴行 (61)
学生の配布資料の利用とそれに依る教育効果の再考永井 喜則 (72)
-

平成21年3月発行

Geometrical Characterization of Textures Consisting of Two or Three Discrete Colorings

Yoshinori Nagai¹, Stephen T. Hyde², Ryan R. L. Taylor³, and Ted Maddess³

(Received 23 January 2009, revised 29 January 2009)

Abstract: Geometrical characterization for discretized contrast textures is realized by computing the Gaussian and mean curvatures relative to the central pixel of a clique and four neighboring pixels, these four neighbors either being first or second order neighbors. Practical formulae for computing these curvatures are presented. Curvatures based on the central pixel depend upon the brightness configuration of the clique pixels. Therefore the cliques are classified into classes by configuration of pixel contrast or coloring. To look at the textures formed by geometrically classified cliques, we create several textures using overlapping tiling of cliques belonging to a single curvature class. Several examples of hyperbolic textures, consisting of repeated hyperbolic cliques surrounded by non-hyperbolic cliques, are presented with the non-hyperbolic textures. We also introduce a system of 81 rotationally and brightness shift invariant geo-cliques that have shared curvatures and show that histograms of these 81 geo-cliques seem to be able to distinguish isotrigon textures.

Key Words: Gaussian curvature, mean curvature, clique, overlapped tiling, textures, hyperbolic textures, non-hyperbolic textures, discretized triangle surface, isotrigon textures.

1. Introduction

We have been studying isotrigon textures in terms of their organization [1, 2, 3] and discrimination by humans [1, 3]. Here we present another viewpoint that may be applied to isotrigon textures. Any texture has the feature of brightness or coloring of each component pixel. In monotone treatment of textures, a texture is equivalent to a brightness surface. Thus we apply the quantities of surface curvature to texture classification to study the relationship between local curvature changes and texture features that are evident on viewing. As a first step towards understanding the geometrical context of isotrigon textures, we calculate practical forms of Gaussian and mean curvatures that are appropriate for isotrigon textures using formulae for those curvatures [4, 5] that consider the discrete covering of a surface by triangles based on the Gauss-Bonnet theorem [6, 7]. In the present paper we yield an adapted form of Gaussian and mean curvatures to investigate texture geometry in Section 2.

¹ Center for Information Science, Kokushikan University

² Department of Applied Mathematics, Research School of Physical Sciences and Engineering, Australian National University

³ ARC Centre of Excellence in Vision and Centre for Visual Sciences, School of Biological Sciences, ANU School of Biology, Australian National University

In this paper we only address textures where each pixel is discretized into two or three brightness levels or colorings. Those textures are called binary textures, when they are defined by two levels of brightness, and ternary textures when they consist of three levels of brightness. As can be easily seen from minimal consideration, any binary texture has no hyperbolic configurations based upon local pixel brightness. Hyperbolic features can only be seen when each pixel can adopt three or more brightness levels. From a visual standpoint this corresponds to 3 contrast levels. Therefore we examine several examples of ternary hyperbolic textures. Section 3 is devoted to the classification of local pixel configurations with respect to nearest neighbor pixels, and second neighbor pixels, and to counting the number of members belonging to the classified classes.

As a partial examination of what can be determined by considering curvature we create some example textures using an overlapping tiling method to illustrate what feature can be seen in such clique-tiled textures. We show several examples of *clique-tiled* textures where the cliques are drawn from classes that are defined by the geometrical sense of pixel contrast configurations. We call the member cliques belonging to the same class classified in the geometrical sense a *geo-clique*. Here we only show tiled textures that use a single class of geo-cliques. Section 4 is a texture gallery to show binary textures tiled by geo-cliques, and a several examples of hyperbolic ternary textures and these are compared with non-hyperbolic ones.

We introduce a method for counting the geo-cliques in Section 5. This method seems to be able to distinguish isotrigran textures.

We discuss the geometrical approach to the isotrigran textures to discriminate those organized by cliques of different configurations contrast with respect to the pixels of the clique, in Section 6.

2. Mathematical foundations for local curvatures of discrete mesh surface

Textures are organized based on a two dimensional arrangement of pixels where brightness is defined for every pixel as shown in Fig. 1, and where each brightness can be thought of as the height of a peak on a rough surface. As shown in Fig. 1, each brightness peak can be connected by a virtual line to form a surface consisting of triangles. If the pixel size becomes infinitely small, the surface formed by the triangles turns into a continuous surface as far as any pixel is not singular against the brightness of neighbor pixels.

The Gaussian and mean curvatures are defined on the continuous surface [6, 7]. The procedure for calculating curvatures using a triangle covering of surfaces gives the curvatures at the point which is at the center of triangles covering local areas. When we use finite sized triangles, we can define the Gaussian and mean curvatures on a surface covered with finite size triangles. The point surrounded by four triangles in Fig. 2(a) is relevant for textures where we define the curvature quantities on the central pixel and its surrounding neighboring four pixels.

We define Gaussian curvature and mean curvature for discrete meshes surface are as fol-

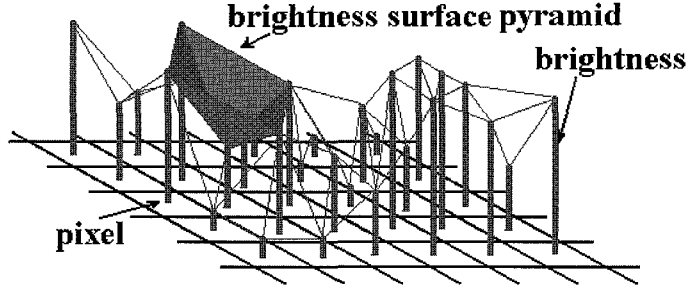


Fig. 1 Schematic illustration of a brightness surface on two-dimensional pixel lattice

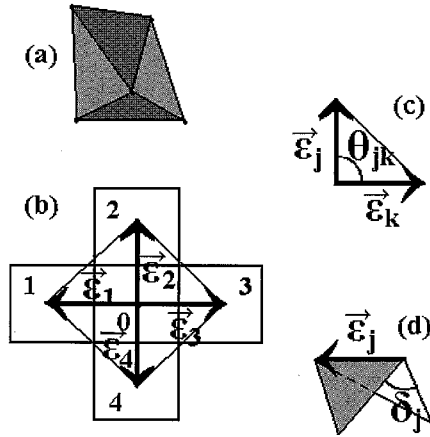


Fig. 2 Definition of vectors (b), angles between vectors (c), and surface angles between neighboring triangular surfaces (d) for a selected local surface patch of brightness pyramid (a)

lows [4, 5].

Gaussian curvature

$$K = \frac{3 \left(2\pi - \sum_{(j,k)} \theta_{jk} \right)}{\sum_{(i,j)} A_{jk}} \quad (2.1)$$

Mean curvature

$$H = \frac{3 \sum_j (\pi - \delta_j) l_j}{4 \sum_{(j,k)} A_{jk}} \quad (2.2)$$

where $(j, k) \in \{(1, 2), (2, 3), (3, 4), (4, 1)\}$, $j \in \{1, 2, 3, 4\}$, where the angles are calculated using vectors bridging between neighbor pixels and their center pixel. K and H are characteristics of the central pixel surrounded by its four neighboring pixels. The above formulae are

obtained from the Gauss-Bonnet theorem [6, 7]. Here we note that

$$l_j = |\bar{e}_j|. \tag{2.3}$$

The angles and areas of triangles appearing in eqs. (2.1) and (2.2) can be described using vectors defined in Fig. 2 as follows.

$$\theta_{jk} = \tan^{-1} \left(\frac{|\sqrt{|\bar{e}_j|^2 |\bar{e}_k|^2 - (\bar{e}_j \cdot \bar{e}_k)^2}|}{(\bar{e}_j \cdot \bar{e}_k)} \right) \tag{2.4}$$

$$A_{jk} = \frac{1}{2} |\bar{e}_j \times \bar{e}_k| \tag{2.5}$$

$$\pi - \delta_j = \sigma_j \tan^{-1} \left(\frac{\sqrt{|\bar{e}_i \times \bar{e}_j|^2 |\bar{e}_j \times \bar{e}_k|^2 - ((\bar{e}_i \times \bar{e}_j) \cdot (\bar{e}_j \times \bar{e}_k))^2}}{(\bar{e}_i \times \bar{e}_j) \cdot (\bar{e}_j \times \bar{e}_k)} \right) \tag{2.6}$$

$$\sigma_j = \frac{\bar{e}_j \cdot ((\bar{e}_i \times \bar{e}_j) \cdot (\bar{e}_j \times \bar{e}_k))}{|\bar{e}_{ji}| |(\bar{e}_i \times \bar{e}_j) \times (\bar{e}_j \times \bar{e}_k)|} \tag{2.7}$$

More practical formulae for Gaussian and mean curvatures for square mesh pixels are obtained below. The letter a appearing in formulae denotes the size of square pixels, namely, $a \times a$, and I means the amplitude of the brightness and the suffixes give the labeling of the pixels. To calculate the curvature, the contrast of brightness is used. So the difference of brightness intensity between center and neighboring pixels gives the vector from the center to the specified pixel neighbors. Thus the quantity ΔI is utilized. For many practical cases a can be taken to be 1.

Gaussian and mean curvatures for the nearest neighbor configuration

$$K = \frac{6 \left(2\pi - \sum_{(j,k)} \tan^{-1} \left(\frac{\sqrt{1 + \frac{\Delta I_j^2 + \Delta I_k^2}{a^2}}}{\frac{\Delta I_j \Delta I_k}{a^2}} \right) \right)}{a^2 \sum_{(j,k)} \sqrt{1 + \frac{\Delta I_j^2 + \Delta I_k^2}{a^2}}} \tag{2.8}$$

$$H = \frac{3}{2} \frac{\sum_j \sqrt{1 + \frac{\Delta I_j^2}{a^2}} \tan^{-1} \sqrt{\frac{\left(1 + \frac{\Delta I_{j-1}^2 + \Delta I_j^2}{a^2}\right) \left(1 + \frac{\Delta I_j^2 + \Delta I_{j+1}^2}{a^2}\right)}{1 + \frac{\Delta I_j^2 - \Delta I_{j-1} \Delta I_{j+1}}{a^2}} - 1}{a \sum_{(j,k)} \sqrt{1 + \frac{\Delta I_j^2 + \Delta I_k^2}{a^2}}} \tag{2.9}$$

Note that K denotes the Gaussian curvature and H the mean curvature. In the Gaussian curvature formula, the dominator includes \tan^{-1} which becomes 0 at an angle of $\pi/2$. If the brightness differences between pixels are zero, both the Gaussian and mean curvatures are zero, i.e., indicating a flat brightness surface. If the brightness differences of neighboring pix-

els have opposite signs, the value of arctangent is larger than $\pi/2$. This case gives negative Gaussian curvature indicating a hyperbolic surface.

Gaussian and mean curvatures for the second neighbor configuration

Thus far we have considered first order neighboring pixels as is generally defined for four-way connectedness. We now consider curvatures for second order pixels that are considered in cases of eight-way connectedness.

$$K = \frac{3 \left(2\pi - \sum_{(j,k)} \tan^{-1} \left(\frac{\sqrt{1 + \frac{\Delta I_j^2 + \Delta I_k^2}{2a^2}}}{\frac{\Delta I_j \Delta I_k}{2a^2}} \right) \right)}{a^2 \sum_{(j,k)} \sqrt{1 + \frac{\Delta I_j^2 + \Delta I_k^2}{2a^2}}} \quad (2.10)$$

$$H = -\frac{3}{4} \frac{\sum_j \sqrt{1 + \frac{\Delta I_j^2}{2a^2}} \tan^{-1} \sqrt{\frac{\left(1 + \frac{\Delta I_{j-1}^2 + \Delta I_j^2}{2a^2}\right) \left(1 + \frac{\Delta I_j^2 + \Delta I_{j+1}^2}{2a^2}\right)}{1 + \frac{\Delta I_j^2 - \Delta I_{j-1} \Delta I_{j+1}}{2a^2}} - 1}{a \sum_{(j,k)} \sqrt{1 + \frac{\Delta I_j^2 + \Delta I_k^2}{2a^2}}} \quad (2.11)$$

The curvatures for a clique of second neighboring pixels are obtained by replacing a^2 by $2a^2$ and the constant pre-factor is twice those for the nearest neighbor case. This is a consistent result since the distance between square pixels becomes $\sqrt{2}a$.

3. Classification of configuration arrangements of brightness for neighboring pixels

The locally hyperbolic or pyramidal surface features of motifs are uniquely determined depending on the configuration of pixel brightness. The local surface features of which motif is hyperbolic or pyramid is uniquely determined depending on the configuration of pixel brightness. Thus the qualitative nature of local surface curvatures can be seen in the configuration of pixels within small cliques. We present here the classification of geometrical features for local brightness surfaces based on 3×3 pixel cliques. This classification of these cliques will be helpful to research the nature of textures.

In the classification, a class is defined as a symbolic clique that is essentially different to each other by any operation where brightness level is shifted and or the clique is rotated. Thus the members of each class are the cliques that coincide to the symbolic clique by brightness shifts and neighboring pixel rotations. The total number of cliques consisting of a center pixel and its surrounding four pixels is $2^5 = 32$ for binary textures and $3^5 = 243$ for ternary tex-

tures. Ternary textures include binary textures of two paired brightnesses of three so that the truly ternary cliques become $3^5 - 81 = 162$. Notice that 81 is the number of different binary cliques in ternary textures. We call the symbolic cliques *geo-cliques* since each clique is vested the quantities of Gaussian and mean curvatures following their pixel brightness configurations.

To organize tables, we adopt the following shorthand names for particular centre versus surround pixel configurations: FP flat plane, BP binary plane, BE binary eagle, BB binary butterfly, BH binary helmet, BY binary yacht, in Table 1, TF ternary flat plane, TP to TY are ternary case of BP to BY in Table 2, and TD ternary doll, TS ternary saddle, TN ternary nipper, TK ternary kite, TC ternary car, TF ternary fish, TA ternary airplane, TB ternary bulldozer, TG ternary goldfish, in Table 3. We additionally give the following definitions for surface motifs or shapes: FPS1 indicates a flat plane of one surface, PS4s a symmetrical four sided pyramidal surface, PS4d a dissymmetric four sided pyramidal surface, BVS2 a butterfly shape V form two-plane, PS4f1 a four sided pyramid of one triangle sit down, PS4u a uneven four sided pyramid, FS2f1 a fence wall shape of two flat plane of one side sit down, ATB arched tail bird, SFP slanting flat plane, ODB one-side dwarf butterfly, WS4t warped surface covered with 4 triangles.

Table 1 Classification of brightness shape configurations for four neighbored pixels in binary textures

class	Nearest neighbor configurations	Second neighbor configurations	Number of class members (total number is 32)	Surface motif	Curvatures	
					Gaussian curvature K	Mean curvature H
1 FS			2	FPS1	K=0	H=0
2 BP			2	PS4s	K>0	H≠0
3 BE			8	PS4d	K>0	H≠0
4 BB			4	BVS2	K>0	H=0
5 BH			8	PS4f1	K>0	H≠0
6 BY			8	FS2f1	K>0	H=0

Notice that the geo-cliques defined here exploit two forms of symmetry: rotational shifts and brightness shifts. In the case of brightness shifts if a gray pixel has a value of i then the white pixel has a value of $\text{modulo}_2(i+1)$, since these are binary textures.

Table 2 Geometrical classification of binary class elements of ternary textures

class	Nearest neighbor configurations	Second neighbor configurations	Number of class members (binary ones in ternary are 81)	Surface motif	Curvatures	
					Gaussian curvature K	Mean curvature H
1 TF			3	FPS1	$K=0$	$H=0$
2 TS			6	PS4s	$K>0$	$H\neq 0$
3 TE			24	PS4d	$K>0$	$H\neq 0$
4 TB			12	BVS2	$K>0$	$H=0$
5 TH			12	PS4f1	$K>0$	$H\neq 0$
6 TY			24	FS2f1	$K>0$	$H=0$

Notice that in this case if the three brightness if a gray pixel has a value of i then the white pixel has a value of $\text{modulo}_3(i+1)$ and the dotted pixels $\text{modulo}_3(i+2)$, since these are ternary textures.

4. Overlapped tiling textures using single cliques classified by their geometrical configuration

We now provide some example textures that each illustrate a single mean and Gaussian curvature by virtue of being compressed of one type of clique only. Those textures are organized by overlap-tiling of a single geo-clique. The overlap-tiling is a procedure to form a texture where each pixel with four neighboring pixels takes the same class configuration of pixel brightness. As mentioned in the previous section each class has the members which coincide with brightness shifts and neighboring pixel rotations. Thus each pixel of the organized texture has the different member of the same class. This manner implies overlap-tiling because the surrounding pixels become a central pixel of next step in the covering geo-cliques. Fig. 3 shows binary overlap-tiling textures using single class of clique for 6 classes of binary geo-cliques. The binary textures organized in this way are quite simple as seen in Fig. 3.

More than 3 brightness levels occur in hyperbolic geo-cliques. Here we show a few examples of textures of which many geo-cliques are hyperbolic. We call those textures *hyperbolic textures*. It is hard to organize textures where every pixel configuration is hyperbolic. A hyperbolic texture includes hyperbolic geo-cliques and non-hyperbolic cliques. *Non-hyper-*

Table 3 Geometrical classification of essentially ternary configurations of elementary neighborings

class	Nearest neighbor configurations	Second neighbor configurations	Number of class members and subclass members	Surface motives	Curvatures		
					Gaussian curvature K	Mean curvature H	
7 TD			24	16	PS4d	$K > 0$	$H \neq 0$
				8	ATB	$K < 0$	$H \neq 0$
8 TS			6	4	PS4m	$K > 0$	$H \neq 0$
				2	Saddle	$K < 0$	$H \neq 0$
9 TN			12	8	PS4d	$K > 0$	$H \neq 0$
				4	SFP	$K = 0$	$H = 0$
10 TK			12	8	ODB	$K > 0$	$H = 0$
				4	SFP	$K = 0$	$H = 0$
11 TC			24	16	PS4u	$K > 0$	$H \neq 0$
				8	WS4	$K < 0$	$H \neq 0$
12 TF			24	19	PS4u	$K > 0$	$H \neq 0$
				8	ATB	$K < 0$	$H \neq 0$
13 TA			12	8	PS4u	$K > 0$	$H \neq 0$
				4	ATB	$K < 0$	$H \neq 0$
14 TB			24	16	PS4u	$K > 0$	$H \neq 0$
				8	WS4	$K < 0$	$H \neq 0$
15 TG			24	16	PS4d	$K > 0$	$H \neq 0$
				8	WS4	$K < 0$	$H \neq 0$

abolic textures in each of which any pixel is non-hyperbolic geo-cliques are possible. We show hyperbolic texture examples together with non-hyperbolic textures of the same class of geo-cliques in order to compare hyperbolic texture with non-hyperbolic textures. Fig. 4 shows those examples. If we take three levels three integers $\{-1, 0, 1\}$, the hyperbolic textures are zero average textures where average is taking over entire pixels. Some examples of hyperbolic textures yield as sense of depth on viewing.

5. Geo-clique histograms of isotrignon textures

For ternary textures if we define modulo₃ based symmetrical forms of the geo-cliques then there are 81 such geo-cliques. For example for the bottom right geo-clique of Fig. 4 has four modulo₃ equivalent forms:

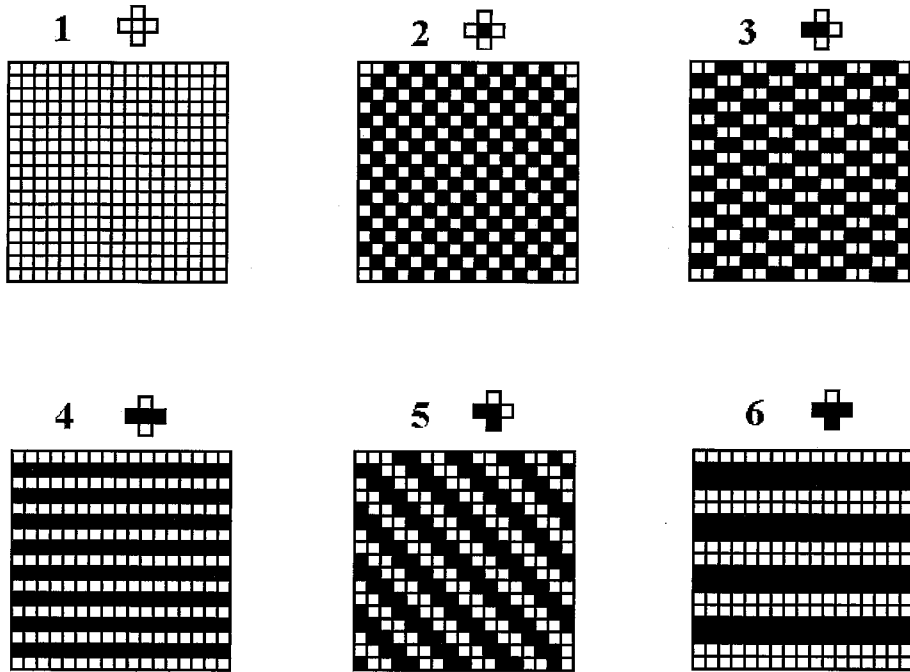


Fig. 3 Binary textures of overlapped tiling only using single geo-clique

1	2	0
0 0 2,	1 1 0,	2 2 1.
0	1	2

and each has four rotational variants, so there are a total of $81 \cdot 3^4 = 972$ geo-cliques that reduce to 81 employing the symmetries of brightness shift and rotation.

We have previously shown [3] that isotricon textures of about 3×3 pixels square are excellent exemplars of their whole class since they will contain all possible cliques in equal numbers, hence they can be thought of as being quite ergodic. We computed histograms of the number of geo-cliques for 5 glider types [1-3] and 6 rules [2, 3], i.e. 30 ternary isotricon texture classes. Fig. 5 illustrates textures created with 5 gliders and 2 rules.

We used 100 examples of each of the 30 types of 3×3 pixel square texture samples. We counted all 972 geo-cliques in each. This was done for first order neighboring pixels (N1) and second order neighboring pixels (N2). This made the histograms for each texture type 4 dimensional. For the purposes of presentation we present averaged histograms, with the averages computed over the 4 rotations, or the 3 brightness shifts, or both. Fig. 6 shows one example for the Box texture type illustrated at top left in Fig. 5.

An interesting feature of Fig. 6 is that the 2D histograms are quite flat across rows, making the 1D histograms reasonable summaries. Interestingly the Box textures for the first 3

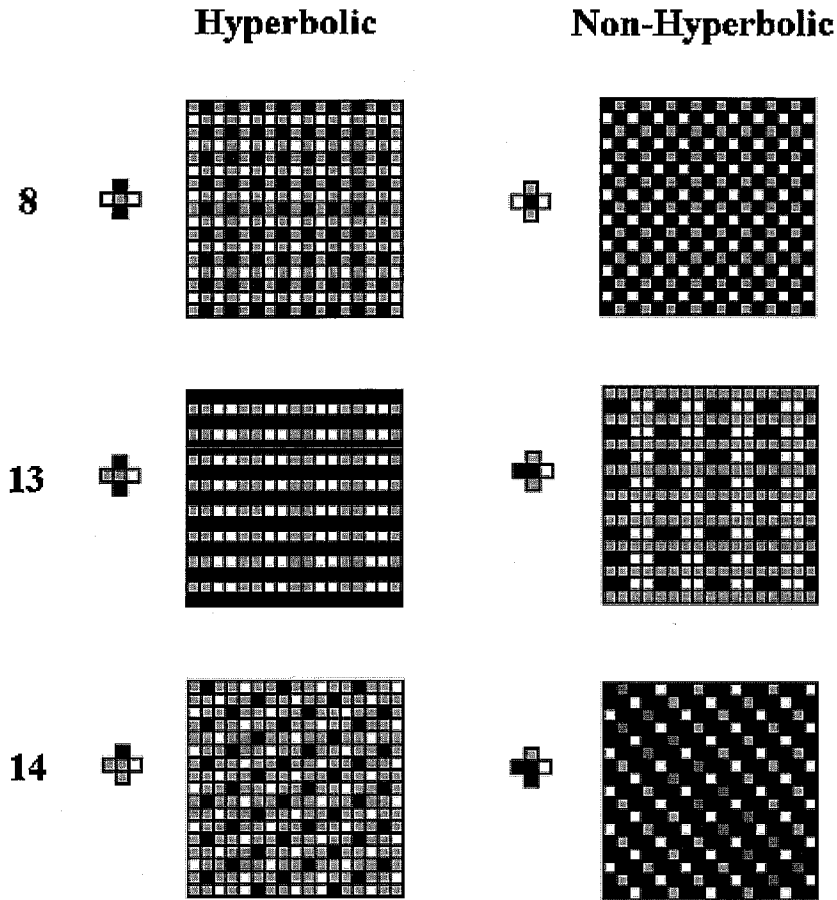


Fig. 4 Hyperbolic ternary textures comparing with non-hyperbolic ones all composed of repeated tilings of the one clique that has a particular mean and Gaussian curvature.

rules only had 27 non-zero N2 geo-cliques. Moreover, these were the same non-zero bins for all three of these rules. Thus the distinguishing features are the N1 histograms. The different levels in the N1 histograms are significant because the standard errors in the bin heights are all close to 0.04 while the bin count values are in the range 3 to 10 geo-cliques per 3×3 pixel square texture example. Other textures had N1 and N2 histograms that were all non-zero such as Fig. 7 for a Zigzag texture.

6. Summary and Discussion

A method for assessing the mean and Gaussian curvature of textures composed of discrete brightnesses or colorings is introduced. We illustrate some of the features of texture surfaces by constructing textures that are repeated tilings of a single clique that illustrate

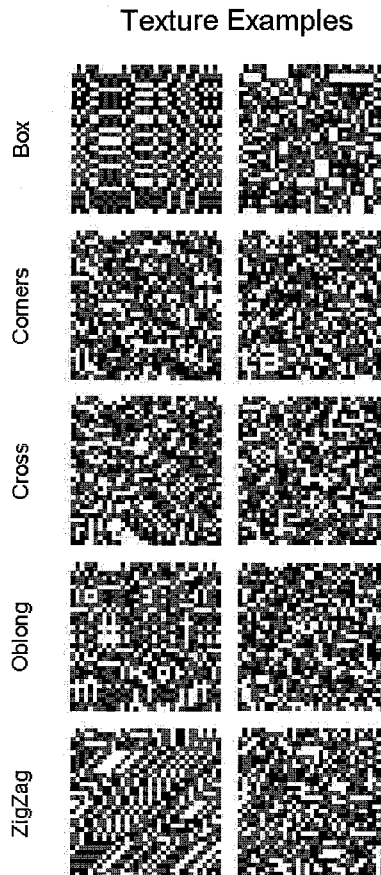


Fig. 5 Examples of the isotrigon textures using in the histogram process. The ordinate labels describe the glider type used. The columns correspond to two different rules.

some particular universal curvature relationships across the textures. We also define a relatively small set of geotextures, 81 when brightness and rotational symmetries are employed. These seem to be able to distinguish isotrigon textures. This may not be completely surprising because while isotrigon textures have 0 average spatial correlation up to third order [2, 3], the present measures are basically 5th order, and so in principle can potentially be used to distinguish these textures. In future work we will examine how the density of hyperbolic and non-hyperbolic geo-cliques varies across these and other images, including natural images. It is possible that hyperbolic configuration of some cliques causes difficulties for the discrimination of textures.

If we utilize the procedure of local structures searching on texture in discriminating textures, samplers similar to the clique consisting of second neighboring pixels will yield better performance based on Taylor's work [8]. Isotrigo texture discrimination depends ultimately upon the pixel brightness arrangements. Thus, one might expect that discrimination would

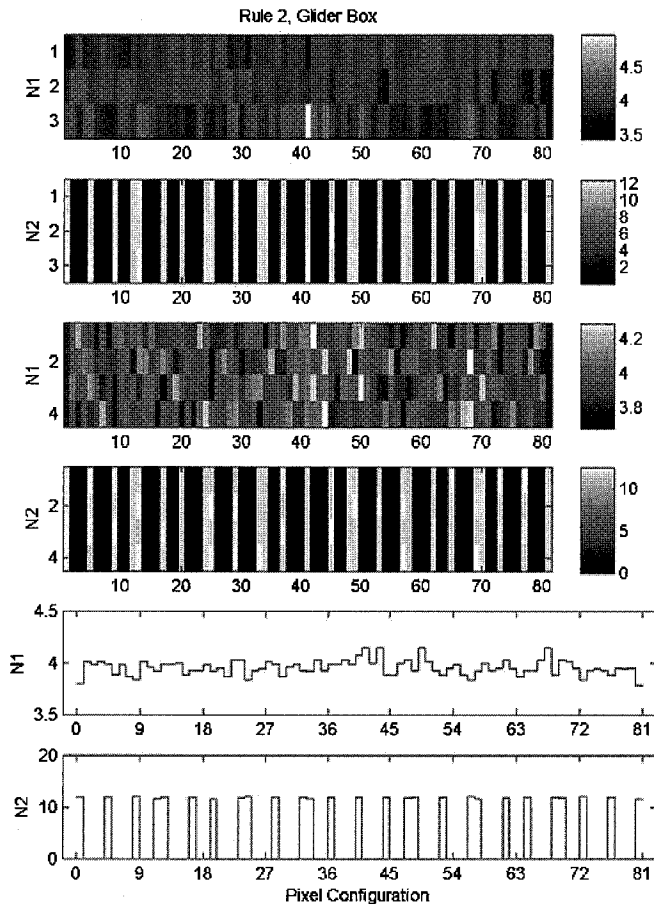


Fig. 6 Averaged histograms for a class of ternary Box textures. The top two histograms are computed only for N1 or N2 neighbor geo-cliques averaging over the four rotations, leaving one row of each histogram for one of the three brightness shifts. The top row corresponds to a central pixel value of 0, the next two rows central values of 1 or 2. The central two histograms are averaged across the three brightness shifts leaving 4 rows corresponding to the 4 rotations. The bottom pair of 1D histograms are averages across both brightness shift and rotation.

be easier when geo-cliques histograms are very different to each other. As seen from Figs. 6 and 7, the cliques of second order neighboring pixels (N2) shows obviously different histograms to each other between Box and Zigzag glider textures. The Box glider geo-clique histogram shows a sparse feature. This may correspond to the lattice feature that clearly appears in binary Box textures. The second neighbor geo-clique can recover this feature in ternary Box textures.

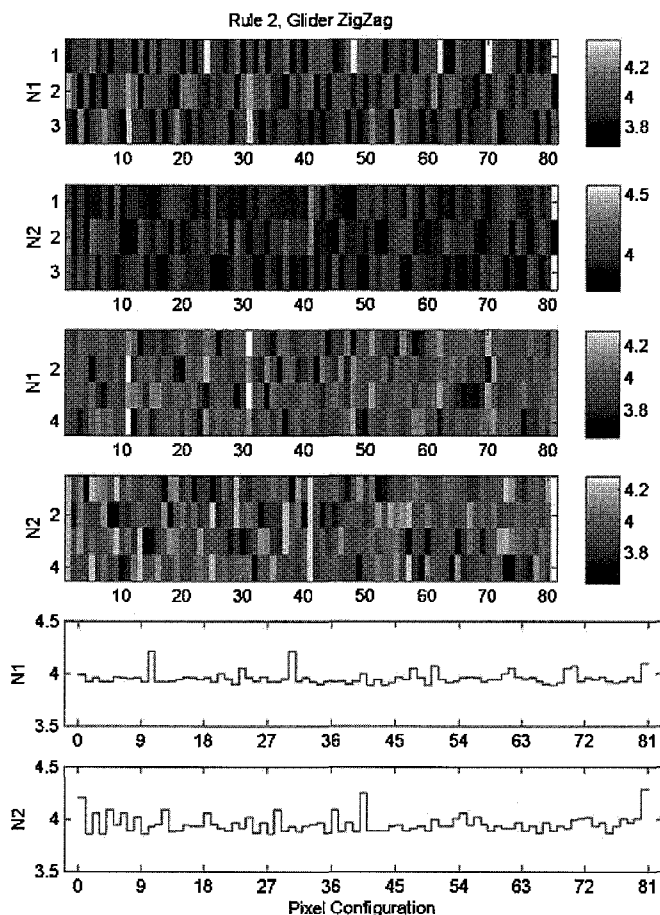


Fig. 7 Averaged histograms for a class of ternary Zigzag textures. The histograms showed some clear peaks that were different than for other isotrignon textures.

References

- [1] Maddess, T., Nagai, Y., Discriminating isotrignon textures, *Vision Res.* **41** (2001) 3837–3860.
- [2] Maddess, T., Nagai, Y., James, A. C., Ankiewicz, A., Binary and ternary textures containing higher-order spatial correlations, *Vision Res.* **44** (2004) 1093–1113.
- [3] Maddess, T., Nagai, Y., Victor, J. D., Taylor, R. R. L., Multi-level isotrignon textures, *J. Opt. Soc. Am. A* **24** (2007) 278–293.
- [4] Hyde, S.T., Ninham, B.W., and Zemb, T., Phase boundary for ternary microemulsions. Predictions of a Geometric Model. *J. Phys. Chem.* **93** (1989) 1464–1471.
- [5] Hyde, S.T., Barnes, I.S., and Ninham, B.W., Curvature energy of surfactant interfaces confined to the plaquettes of a cubic lattice. *Langmuir* **6** (1990) 1055–1062.
- [6] doCarmo, M., *Differential Geometry of Curves and Surfaces*. Englewood Cliffs, N. J., Prentice-Hall Inc, 1976.
- [7] Kreyszig, E., *Differential Geometry*, Dover edition, Dover, 1991.
- [8] Taylor, R. R. L., Maddess, T., Nagai, Y., Spatial biases and computational constraints on the encoding of complex local imaging structure, *J. Vision* **19** (2008) 1–13.